Numerical Simulation of Ice Cover of Saline Lakes

V. M. Stepanenko[a], *, I. A. Repina[a, b], G. Ganbat[c], and G. Davaa[c]

[a]*Moscow State University, Moscow, Russia*
[b]*Obukhov Institute of Atmospheric Physics, Russian Academy of Sciences, Moscow, Russia*
[c]*Information and Research Institute of Meteorology, Hydrology and Environment, Ulaanbaatar, Mongolia*
***e-mail: stepanen@srcc.msu.ru*

Abstract—A new version of the one-dimensional thermo-hydrodynamic and biogeochemical model LAKE2.1 is presented. The model is supplemented with a description of the dynamics and vertical distribution of salinity in an ice cover. Simulation results are compared to in situ and satellite data of water temperature and ice cover at Uvs Nuur Lake (Mongolia) from 2000 to 2015. It is shown that underestimating the mixed-layer depth by the model with standard turbulence closure $k-\varepsilon$ during summer and autumn leads to a significant shift in the timing of the onset of ice. It is also demonstrated that, while neglecting the salinity of the lake, the freeze-up according to the model happens 16–17 days earlier than in reality. This error is removed if the effect of salinity on water density and freezing temperature is included. However, in this case, the model underestimates the maximal seasonal ice thickness on average by ≈0.2 m. In turn, this error decreases an order of magnitude if the dynamics and vertical distribution of salinity in ice are simulated in the model.

INTRODUCTION

The ice regime is the crucial characteristic of inland water bodies. The onset of the ice cover stops the flux of momentum into the reservoir from the atmosphere, which leads to the establishment of an almost laminar flow regime and weak molecular vertical diffusion. A sharp reduction in solar radiation shifts the ecosystem functioning into the winter mode. The lack of connection with the atmosphere decreases the concentration of oxygen in water due to its consumption by decomposition of organic compounds [1]. With sufficiently long freeze-up, this can lead to high fish mortality. Simultaneously with the decrease in the concentration of oxygen, the content of methane and carbon dioxide, which are greenhouse gases, increases and they will be released into the atmosphere during ice-off [2]. The ice-off time also determines the beginning of mixed-layer temperature rise in the reservoir and, therefore, the temperature of this layer in the first half of summer. Under modern climate change, the ice-off time is noticeably reduced [3, 4], which increases the relevance of studying the physical mechanisms of ice formation and the destruction of the ice cover.

Large literature is devoted to the mathematical modeling of the ice regime of inland waters. All models the authors are aware of are one-dimensional. The basis of these models is the solution of the heat transport equation with a radiation source, solved in snow and ice with the corresponding boundary conditions.

The heat transfer in the water layer is of secondary importance for this task, since the heat flux below the freezing front is usually small and may not be taken into account in the first approximation. In a number of models, the stationary version of the heat equation in snow and ice covers is solved [5]. Excluding the volume absorption of radiation, this approximation gives a linear temperature profile in both layers [6]. In most models, the heat equation is solved in a complete nonstationary form by finite difference methods [7–10].

Much less attention is paid in the literature to the numerical simulation of the thermodynamic and ice regime of salt lakes than to the modeling of freshwater objects. The few works devoted to the calculation of the evolution of the ice cover in salt lakes [10] do not take into account the effects of the "capture" of salt water in the pores of the growing ice cover—a phenomenon well studied for the sea ice [11]. However, it is not pertinent to apply models developed for the formation of sea ice to lakes, since, unlike lake ice, sea ice moves under the influence of wind and currents, the divergence and convergence of which leads to the formation of significant spatial variability of ice concentration; therefore, rather complicated equations of ice-cover dynamics are used in the corresponding models [12, 13].

This article presents a new version of the one-dimensional thermo-hydrodynamic LAKE 2.1 model of the water reservoir [14, 15], in which the ice-cover block is supplemented with a description of the salinity

evolution. The model is verified with the use of observational data collected for the Uvs Nuur Lake (Mongolia) and the effect of salinity on the lake's ice regime is estimated.

DESCRIPTION OF THE MODEL

General Characteristics of the Model

The one-dimensional LAKE model of thermohydrodynamics and biogeochemistry of the reservoir and underlying sediments [14−16] includes the processes of vertical heat transfer, taking into account the propagation of shortwave radiation in the layers of water, ice, snow, and bottom sediments. The model equations are formulated with respect to values averaged over the horizontal cross-section of the reservoir, which leads to an explicit accounting for the momentum, heat, and solutes exchange between the water medium and the sloping bottom. In the water column, $k-\varepsilon$ parametrization of turbulence is used, and the equations of motion allow for the inclusion of the barotropic pressure gradient [15]., which is not used in this study In the snow layer, the vertical transfer of liquid moisture is taken into account, and the possibility of its freezing is implemented in the soil layer. The model describes the vertical diffusion of dissolved gases CO_2, CH_4, and O_2, as well as their bubble transfer, production and oxidation of methane, photosynthesis, and processes of oxygen consumption. The model was tested in the ability to reproduce the thermal and ice regimes of a large number of reservoirs in contrasting climatic conditions, including those studied in the framework of the LakeMIP project (Lake Model Intercomparison Project, [17−20]).

Transfer of Heat and Salinity in the Ice Cover

In the LAKE 2.0 version of the model, ice is considered fresh and its thermophysical properties are homogeneous vertically. In fact, ice always contains pores occupied by gases or liquid water. In version 2.1, the porosity of ice is introduced, which is occupied only with liquid water containing dissolved salts. The ice porosity p due to the water content is defined as

$$p = \frac{V_w}{V_w + V_i}, \tag{1}$$

where V_w is the brine volume and V_i is the volume of clear ice. The volume heat capacity $\rho_i c_i$ and the thermal conductivity λ_i of porous ice are calculated according to the volume fractions of water and ice [21]:

$$\rho_i c_i = (1 - p)\rho_{i0} c_{i0} + p\rho_{w0} c_{w0}, \tag{2}$$

$$\lambda_i = (1 - p)\lambda_{i0} + p\lambda_{w0}, \tag{3}$$

where ρ is the density; c is the specific heat; and indices $w0$ and $i0$ correspond to the reference values of the thermodynamic characteristics for water and pure ice, respectively. The effect of the salinity of pore water on

the heat capacity and thermal conductivity of this water is neglected.

The heat conduction equation averaged over the horizontal section of a water body in a layer of porous ice using the normalized vertical coordinate $\xi = z/h_i(t)$ has the following form [15]:

$$\rho_i c_i \frac{\partial T}{\partial t} = \underbrace{\rho_i c_i \frac{\xi}{h_i} \frac{dh_i}{dt} \frac{\partial T}{\partial \xi}}_{I} - \underbrace{\rho_i c_i \frac{1}{h_i} \frac{dh_{i0}}{dt} \frac{\partial T}{\partial \xi}}_{II} - \underbrace{\frac{1}{h_i} \frac{\partial S}{\partial \xi}}_{III}$$

$$+ \underbrace{\frac{1}{Ah_i^2} \frac{\partial}{\partial \xi}\left(A\lambda_i \frac{\partial T}{\partial \xi}\right)}_{IV} + \underbrace{\frac{1}{Ah_i} \frac{\partial A}{\partial \xi} F_{T,b}}_{V} - \underbrace{L\rho_i \frac{\partial p}{\partial t}}_{VI}. \tag{4}$$

Here, z is the coordinate directed along gravity with the beginning on the ice surface, h_i is ice thickness, T is temperature, dh_{i0}/dt is the increment of ice thickness on its surface, S is the shortwave radiation flux (the weakening of which in layers of snow, ice, and water is calculated according to the Beer−Bouguer−Lambert law), L is the freezing/thawing heat of water, A is the z-dependent cross-sectional area of the ice cover determined by the lake basin morphometry, and $F_{T,b}$ is the heat flux at the ice− sediment boundary. The heat flux $F_{T,b}$ is calculated by invoking the solution of one-dimensional heat conduction problems in columns of bottom sediments lowered down from different depths of the lake [15]. This paper uses five such columns. The metric items I and II appeared due to the use of the normalized vertical coordinate and the movement of the origin of coordinates during ice growth/thawing at its upper boundary. The VI term is responsible for the release/absorption of heat during the freezing/thawing of water contained in brine.

Note that the I and II items in Eq. (4), which are not taken into account in virtually all lake models , are not negligible. It is easy to show that

$$\frac{I}{IV} \sim \frac{II}{IV} \sim \frac{h_i^2 \rho_i c_i}{t_i \lambda_i} \approx \frac{1}{7}, \tag{5}$$

where t_i is the time during which ice with thickness h_i. was formed. In the estimate above, the values $h_i = 1$ m, $t_i = 3$ months, $\lambda_i/(\rho_i c_i) \approx 10^{-6}$ m²/s are used.

Equation (4) requires two boundary conditions. At the $\xi = 0$ boundary, the heat-balance equation is used, or, in the case of snow cover, the continuity of temperature and heat flux at the snow-ice boundary. On the lower surface of the ice, the freezing temperature is assigned, which is determined by the salinity of water at the ice-water boundary.

The density of salts in the ice cover (mass of salts per unit volume of porous ice) ρ_s is related to the porosity of ice p and the concentration of salts in the pore brine ρ_{sp} as

$$\rho_s = \rho_{sp}p. \tag{6}$$

Water freezing in brine involves the formation of pure ice from the water, while the salts remain in the liquid phase. The removal of salts from the ice cover, according to Yu.L. Nazintsev and V.V. Panov [11], occurs due to the following mechanisms:

(1) the molecular diffusion of salts due to the brine concentration gradient in the ice cover;

(2) "pressing out" of the brine onto the ice surface due to internal pressure in the ice cover;

(3) the gravitational runoff of brine along cracks;

(4) the "washout" of brine due to the pressure by the layer of thawed water on the surface of the ice cover.

Mathematically describing these processes is a complex task, which is solved at the parameterization level, for example, in the SAMSIM sea-ice-cover model [13]. In our model, a simple approach is proposed in which the salt discharge from the ice cover due to all the mechanisms described above is assumed to be proportional to ρ_s. This does not allow one to obtain, for example, the well-known "C-shaped" profile ρ_s with a maximum on the ice surface and near the frost boundary in the model [22]; however, it reproduces the general tendency of ice desalination with time throughout the ice profile.

Taking into account the above assumptions, the equation for ρ_s takes the following form:

$$\frac{\partial \rho_s}{\partial t} = \underbrace{\frac{\xi}{h_i} \frac{dh_i}{dt} \frac{\partial \rho_s}{\partial \xi}}_{I} - \underbrace{\frac{1}{h_i} \frac{dh_{i0}}{dt} \frac{\partial \rho_s}{\partial \xi}}_{II} - \underbrace{\alpha \rho_s}_{III}, \tag{7}$$

where term III parameterizes the drain of salts and α is the reciprocal of the characteristic time of the removal of salts. The characteristic time for the removal of salts is assumed to be 1 year on the basis of the well-known fact that 1-year-old sea ice is practically fresh [23].

To solve Eq. (7), one boundary condition is required. This condition should take into account that the salinity of the newly formed ice significantly depends on the rate of advance of the phase transition front [11]. In the model, this physical effect is taken into account as follows:

$$\rho_s|_{\xi=1} = s_0 \max[(p_0 \rho_{w0} + (1 - p_0)\rho_{i0}) f(W),$$
$$\rho_{w0} p_{0,\min}], \tag{8}$$

$$f(W) = \frac{C_1 \sqrt{W}}{C_2 \sqrt{W} + C_3}, \tag{9}$$

where the velocity of the phase front W is expressed in mm/h; $f(W)$ is the empirical dependence of V.L. Tsurikov; $C_1 = 7$, $C_2 = 7$, and $C_3 = 10.3$ are empirical constants; s_0 is the salinity of water at the water–ice binterface as a mass fraction of salts; ρ_{w0} is the average density of water; and $p_{0,\min}$ is the minimum value of ice porosity at this boundary, assumed constant (in the model 0.05). In formula (8), a lower limit is intro-

duced by the quantity $s_0 \rho_{w0} p_{0,\min}$, since V.L. Tsurikov's formula gives zero salinity of ice at zero speed of the front movement. The physical meaning of equality $\rho_s|_{\xi=1} = s_0 \rho_0 p_0$ where $p_0 = p_s|_{\xi=1}$ is that the salt concentration in pores $\rho_{sp}|_{\xi=1}$, which form when the ice cover grows from below, is equal to the salt concentration in the water immediately below the freezing front.

Formulas for calculating the rate of change of ice-cover thickness dh_i/dt, dh_{i0}/dt are given in the next section. To close system of equations (4), (6), (7), one more relation is required, which is the condition of thermodynamic equilibrium:

$$T = T_{fr}(\rho_{sp}), \tag{10}$$

where T_{fr} is the freezing point, determined by the salinity of the brine ρ_{sp}.

The growth and thawing of ice lead to changes in water salinity. In the LAKE model, the salinity of water is calculated based on the vertical diffusion equation:

$$\frac{\partial s}{\partial t} = \underbrace{\frac{\xi_w}{h_w} \frac{dh_w}{dt} \frac{\partial s}{\partial \xi_w}}_{I} - \underbrace{\frac{1}{h_w} \frac{dh_{w0}}{dt} \frac{\partial s}{\partial \xi_w}}_{II}$$
$$+ \underbrace{\frac{1}{Ah_w^2} \frac{\partial}{\partial \xi_w}\left(Ak_s \frac{\partial s}{\partial \xi_w}\right)}_{III} - \underbrace{\int_{\Gamma_{A(z)}} s(\mathbf{u_h} \cdot \mathbf{n})\, dl}_{IV}. \tag{11}$$

Here, s is the salinity of water (mass fraction of salts, kg/kg); h_w is the thickness of water; $k_s = k_{s,m} + k_{s,t}$ is the sum of molecular and turbulent diffusion coefficients, respectively (the latter is calculated using the turbulent closure $k-\varepsilon$), $\xi_w = z_w/h_w(t)$ is the dimensionless vertical coordinate, in which $z_w = 0$ corresponds to the upper boundary of the water layer; $\Gamma_{A(z)}$ is the boundary of the cross-section $A(z)$); $\mathbf{u_h} = (u, v)$ is horizontal flow velocity; n is the outward normal to $\Gamma_{A(z)}$ and dl is the increment of the length of the boundary. Terms I and II are similar to the corresponding terms in Eq. (7). Term IV expresses the transfer of a lake salinity with streams inflowing and flowing out. Equation (11) is written neglecting the flux of salts through the inclined bottom surface.

The effect of the freezing or thawing of ice on the salinity of water is expressed through the upper boundary condition of Eq. (11):

$$-\frac{k_s}{h_w} \frac{\partial s}{\partial \xi_w}\bigg|_{\xi_w=0} = -\frac{dh_{w0}}{dt} s_0$$
$$+ \frac{dh_{w1}}{dt}\left(\frac{\rho_s}{\rho_{w0}}\bigg|_{\xi=1} - s_0\right) + \frac{\alpha h_i}{\rho_{w0}} \int_0^1 \rho_s d\xi. \tag{12}$$

Here, dh_{w0} is a layer of fresh water flowing through the ice cover as a result of melting snow and ice on the surface of the ice cover; dh_{w1} is a layer of water formed as

a result of freezing or melting of the porous ice cover from at its bottom. The third term on the right-hand side of Eq. (12) is the flux of salts due to the brine run-off through cracks in the ice cover. At the bottom of the lake ($\xi_w = 1$), the salt flux is assumed to be zero.

Evolution of Ice Thickness

The increment of ice layer thickness dh_i during time dt consists of the ice increment at the upper boundary dh_{i0} and at the lower boundary dh_{i1}: $dh_i = dh_{i0} + dh_{i1}$. As in the case of phase transitions inside the ice cover, only fresh water is involved in the phase change at both borders of the ice cover.

The thickness increment at the lower boundary is the thickness of the formed or thawed layer of porous ice. The volume of fresh ice V_{ice}^{fr} formed during the freezing of volume of water V_w^{fr} is $V_{ice}^{fr} = V_w^{fr} \rho_{w0}/\rho_{i0}$ The volume of the pores occupied by the brine is given by $V_p = p_0 V_{ice}^{fr}/(1 - p_0)$ (see definition of porosity (1)). Then, for the volume of newly formed porous ice $V_{ice,p}^{fr}$, we get

$$V_{ice,p}^{fr} = V_{ice}^{fr} + V_p = \frac{V_w^{fr} \rho_{w0}}{\rho_{i0}(1 - p_0)}. \tag{13}$$

At the same time, the water column loses a volume equal to the sum of the volume of water turned into ice and the volume of water that has occupied the pores of the ice cover:

$$V_w = V_w^{fr} + V_p = V_w^{fr} \left[1 + \frac{p_0 \rho_{w0}}{\rho_{i0}(1 - p_0)} \right]. \tag{14}$$

Let $dh_{w1,fr}$ be the change in the thickness of the water layer only due to phase transitions at the ice-water interface, i.e., the value of V_w^{fr} per unit area. This increment is determined by the magnitude of the heat flux discontinuity at this boundary:

$$L\rho_{w0} \frac{dh_{w1,fr}}{dt} = -\frac{\lambda_i}{h_i}\frac{\partial T}{\partial \xi}\bigg|_{\xi=1} + \frac{\lambda_w}{h_w}\frac{\partial T}{\partial \xi_w}\bigg|_{\xi_w=0}. \tag{15}$$

It involves λ_w, which is the sum of the coefficients of molecular and turbulent thermal conductivity in water. Using (13) and (14), we get

$$dh_{w1} = dh_{w1,fr}\left[1 + \frac{p_0 \rho_{w0}}{\rho_{i0}(1 - p_0)} \right], \tag{16}$$

$$dh_{i1} = -dh_{w1,fr}\left[\frac{\rho_{w0}}{\rho_{i0}(1 - p_0)} \right]. \tag{17}$$

CHARACTERISTICS OF THE WATER OBJECT AND THE SETUP OF NUMERICAL EXPERIMENTS

Uvs Nuur is the largest lake in Mongolia, with an area of 3350 km², located in the northwest part of the country. The water in the lake is salty. Starting from the second half of the 20th century, the average mineralization of lake waters tended to decrease (from 180 mg/L in 1930 to 140 mg/L in 2000 [24]). The maximum depth of the lake is 22 m. The climate in the lake basin is extremely continental, with a small annual precipitation (143 mm) and a pronounced annual course of air temperature (mean July temperature is 20°C, January is −32°C) [25].

The attenuation coefficient of visible radiation in the water of the lake used in the Beer−Bouguer−Lambert law (0.4 m⁻¹) was obtained using the Poole and Atkins formula [26] by substituting the characteristic Secchi disk depth, which is 5 m [25]. The attenuation coefficient in the ice cover was chosen as 3 m⁻¹ as an estimate of the average value between 1.5 m⁻¹ for clear ice [27] and ice covered with snow, which has optical properties similar to snow (the attenuation coefficient for snow exceeds 1/(20 cm) = 5 m⁻¹, [8]). As an albedo of pure ice, a value of 0.4 was chosen, which is characteristic of a thawing surface [27], since it was during the thawing period that this parameter had the greatest influence on the evolution of ice thickness. The hypsometric curve (the dependence of the cross-sectional area A on z) for the lake is taken from [24]. The influence of the tributaries of the lake, including effects on the salinity of the water, was not taken into account. The parameters of the numerical experiment are given in Table 1.

Three-hour ERA-Interim reanalysis surface data for the years 1979−2015 were used as atmospheric forcing for the lake model: air temperature and humidity, atmospheric pressure, downward shortwave and longwave radiation, precipitation, wind speed and direction. The reanalysis fields were interpolated from four neighboring points to the center of the lake using the bilinear function. Reanalysis data were chosen as covering the largest time interval among the sources available to the authors; in addition, radiation fluxes at standard meteorological stations are not measured.

The following empirical data were used to validate the model:

(1) Measurements of the water-surface temperature at the Davst coastal hydrological station (west coast of the lake, 50.32 °N, 92.29 °E), mean monthly values from 1979 to 2015.

(2) Satellite data on the surface temperature range obtained using a Moderate Resolution Imaging Spectroradiometer (MODIS) scanning spectroradiometer (www.modis.gsfc.nasa.gov, http://ladsweb.nascom.nasa.gov/index.html) installed on the TERRA satellite. The method described in [29] was used to deter-

Table 1. Parameters of numerical experiments with the LAKE 2.1.- model

Parameter	Value	Reference
Parameters of the lake		
Maximum depth of the lake	22 m	[24]
Initial salinity of the water	17‰	[24]
Attenuation coefficient of visible radiation in water	0.4 m^{-1}	[25]
Attenuation coefficient of visible radiation in ice	3 m^{-1}	[8, 27]
Physical parameters		
Albedo of water	0.06	–
Albedo of ice	0.4	[[8, 27, 33]]
Albedo of snow	0.85	–
Numerical implementation parameters		
Model integration period	Jan. 1, 1979 to Dec. 12, 2015	–
Vertical resolution	20 layers	–
Time step	20–30 s	–

mine the surface temperature. In constructing the lake mask, only those pixels that are reliably located on the surface of the lake and do not overlap with the coastal areas were taken into account [30]. Along-Track Scanning Radiometers (ATSRs) and Advanced Along-Track Scanning Radiometers (AATSRs) from the ARC-Lake [31] and Monitoring of IR Clear-sky Radiances over Oceans for SST (MICROS) archives were also involved.

(3) Data on the ice cover are taken from satellite observations in the visible range (2000–2015). The original measurements were obtained using a MODIS scanning spectroradiometer. From 2012 to 2017, the L1C product of the MIRAS microwave radiometer (SMOS/ESA satellite) was also used, which allows one to obtain the seasonal dynamics of the brightness temperature of the geodetic cell corresponding to the Uvs Nuur lake. Periods which are characteristic for open water and ice cover values of the brightness temperature are identified [32].

To assess the influence of the salinity of Lake Uvs Nuur on the ice regime, have been carried out with the LAKE model three main numerical experiments:

(1) the E1 Experiment, in which both water and ice are considered fresh;

(2) the E2 Experiment, in which the salinity of the water is taken into account, but the ice remains fresh ($p = 0$, $\rho_s = 0$); i.e. when ice forms, all salts remain in the water;

(3) the E3 Experiment, in which the salinity of water and ice is calculated using the equations described above in "Description of the model".

The motivation of the E1 experiment is that current weather-forecasting systems and models of the Earth system consider all inland water fresh; therefore, it is important to understand what error this introduces in the calculations of the ice and thermal regime of salt-water bodies. In addition to the experiments mentioned, a calculation was made in which the salinity of

the ice was considered equal to a constant value of 4‰. This value was obtained as a characteristic value for the ice cover of Lake Uvs Nuur based on formulas (8)–(9).

RESULTS AND DISCUSSION

Thermal regime and vertical mixing. In the model calculations, it turned out that the basic version of the LAKE model with a turbulent closure $k-\varepsilon$ generates a very shallow summer mixed layer ($\sim$5 m against $\sim$15 m, according to measurement data, [25]), which is a problem encountered earlier by the authors when applying this model to Lake Baikal (unpublished). This results in the underestimation of the heat content of the lake by the beginning of the autumn period and the hence, faster cooling of the water surface when compared to observations (see the mean surface temperature in October and November in Fig. 1) and a too early onset of ice cover. Figure 1 includes the following empirical data: the temperature observed at the hydrological station and the temperature averaged over all the "lake" pixels of satellite images. It is more correct to compare the results of the model with satellite data, since the model calculates the horizontal average of the surface temperature. The relatively low values of water temperature at the station can be caused by the accelerated cooling of the littoral in autumn known for many water bodies [34].

An analysis of existing approaches to one-dimensional modeling of lakes showed that, at present, the absolute size of the lake is not taken into account explicitly in the equations of thermo-hydrodynamics of these models. Indeed, in the Eq. (4), the term *IV* may be written as

$$\frac{1}{Ah_i^2}\frac{\partial}{\partial\xi}\left(A\lambda_i\frac{\partial T}{\partial\xi}\right) = \frac{1}{h_i^2}\frac{\partial}{\partial\xi}\left(\lambda_i\frac{\partial T}{\partial\xi}\right) + \frac{1}{Ah_i^2}\frac{\partial A}{\partial\xi}\lambda_i\frac{\partial T}{\partial\xi}. \quad (18)$$

Therefore, terms *IV* and *V* of Eq. (4) include only a *relative* decrease in the lake area with a depth dA/dzA^{-1}, while the absolute dimensions of a lake do
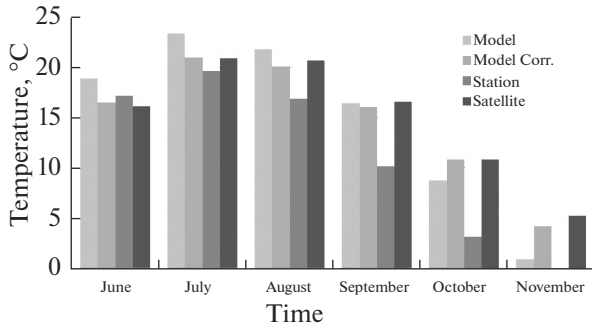
Fig. 1. Mean monthly surface temperature of Lake Uvs Nuur for 2001−2015 according to the results of calculations by the original version of the LAKE model (*Model*), model with the addition of a background diffusivity (*Model Corr.*) according to measurements at the Davst hydrological post (*Station*), and according to the data of temperature recovery from satellite measurements (*Satellite*). The standard deviation of the monthly temperature during 2001−2015 for different months ranges from 0.0 to 1.5°C according to satellite measurements and from to 0.6 to 1.1°C in the model.

not enter governing 1D equations. At the same time, it is well known in limnology that, with an increase in the size of a water body, the depth of the mixed layer, with other conditions unchanged, increases [35, 36]. The literature has long discussed the possible contribution of the collapse of internal waves breaking to the generation of turbulent kinetic energy in a thermocline (see, for example, [37]). For large lakes, it is also possible to use concepts that have been developed in oceanology on the interaction of internal waves and turbulence [38].

To take in account the effect of lake size when its physical mechanisms are poorly understood, empirical corrections to the vertical diffusion coefficient, including the size of the lake in explicit form, for example, M.Hondzo and H.Stefan parametrization [39], have been proposed for one-dimensional models. These authors introduce an additional background diffusion coefficient (thermal diffusivity) in the thermocline:

$$k_{s,b} = k_{T,b} = k_0 A_0^{k_1} \left(N^2 \right)^{k_2}, \quad (19)$$

where A_0 is the surface area of the lake and $k_1 = 0.56$, $k_2 = 0,43$, $k_0 = 8.17 \times 10^{-5}$ cm^2/s are empirical constants. This parameterization was included in the calculation of the diffusion coefficient of the LAKE model, so that

$$k_s = k_{s,m} + k_{s,t} + k_{s,b}, \quad (20)$$

and, similarly, introduced to the calculation of the coefficient of thermal diffusivity during the period of open water, when there is a flux of kinetic energy from the atmosphere, partially transforming into the energy of internal waves. The result was a better reproduction of the annual course of the surface temperature of the lake (Fig. 1) and the vertical temperature profile.

Coefficient k_0 is the only one calibrated in the present work, and its value turned out to be an order of magnitude lower than in [39]. This can be explained by the fact that, in article [39], k_0 was calibrated as part of a model with a fundamentally different vertical mixing scheme, where a bulk model for a mixed layer is used, and coefficient $k_{s,b}$ is introduced as a coefficient of turbulent diffusion in the thermocline, while in the LAKE model $k_{s,b}$ is added to the turbulent diffusion coefficient calculated by the $k-\varepsilon$ model (20).

Ice regime. Figures 2a and 2b show the examples of the evolution of the snow and ice thickness during two different winter seasons. As can be seen from the figures, if we assume that the water in the lake is fresh, the onset of ice happens much earlier (on average more than 2 weeks, see Table 2) than according to observations and E2, E3 experiments. This is caused, on the one hand, by a higher freezing point of fresh water and, on the other, the faster cooling of the surface. With a characteristic lake salinity value of 17 ‰, the temperature of the maximum water density drops to −0.1°C and, by the time the freezing point on the surface ($\approx$−1.13°C) is reached, the lake in experiments E2 and E3 is almost completely mixed vertically. The additional buoyancy flux that occurs when the surface layer is salinized due to autumn evaporation also contributes to mixing. At the same time, in the experiment with fresh water, the cooling of the deep layers stops with a temperature of about 4°C and further cooling of the surface occurs at a faster rate due to a sharp decrease in the depth of the upper mixed layer.

Due to the earlier onset of ice in the E1 experiment, the maximum ice thickness during a winter season, as a rule, is 0.1−0.2 m more than in experiments accounting for salinity, which is illustrated by the winter case of 1993−1994 shown in Fig. 2a. This is also caused by a smaller heat flux from the deep layers of water to the freezing front (5 W/m^2 against 8.4 and 9.3 W m^2 in E2 and E3 experiments, respectively). The greater heat flux when taking into account the salinity of water is due to the fact that the release of salts during the freezing of ice leads to unstable stratification in the upper layers of water and a more intensive exchange of heat with the underlying layers. However, in a number of winter seasons in the E1 experiment, the ice is not the thickest, i.e., in 1996−1997(Fig. 2b). In these cases, after the onset of ice in the E1 experiment and before the start of freeze-up in the E2 and E3 calculations, the snow falls. Due to thewell- known thermal insulation by the snow cover, the rate of ice growth drops sharply in the E1 calculation and, as a result, the maximum thickness of ice is achieved in the E3 experiment. The ice grows more in the E3 experiment than in the E2 one throughout all years of calculation (Fig. 2). This is partly due to the earlier date (on average, by 1.6 days, Table 2) of the onset of ice cover in E3 calculations. In addition, using formula (17), it is easy to show that $dh_{i1,E3}/dh_{i1,E2} \approx 1/(1-p_0))$ with the same
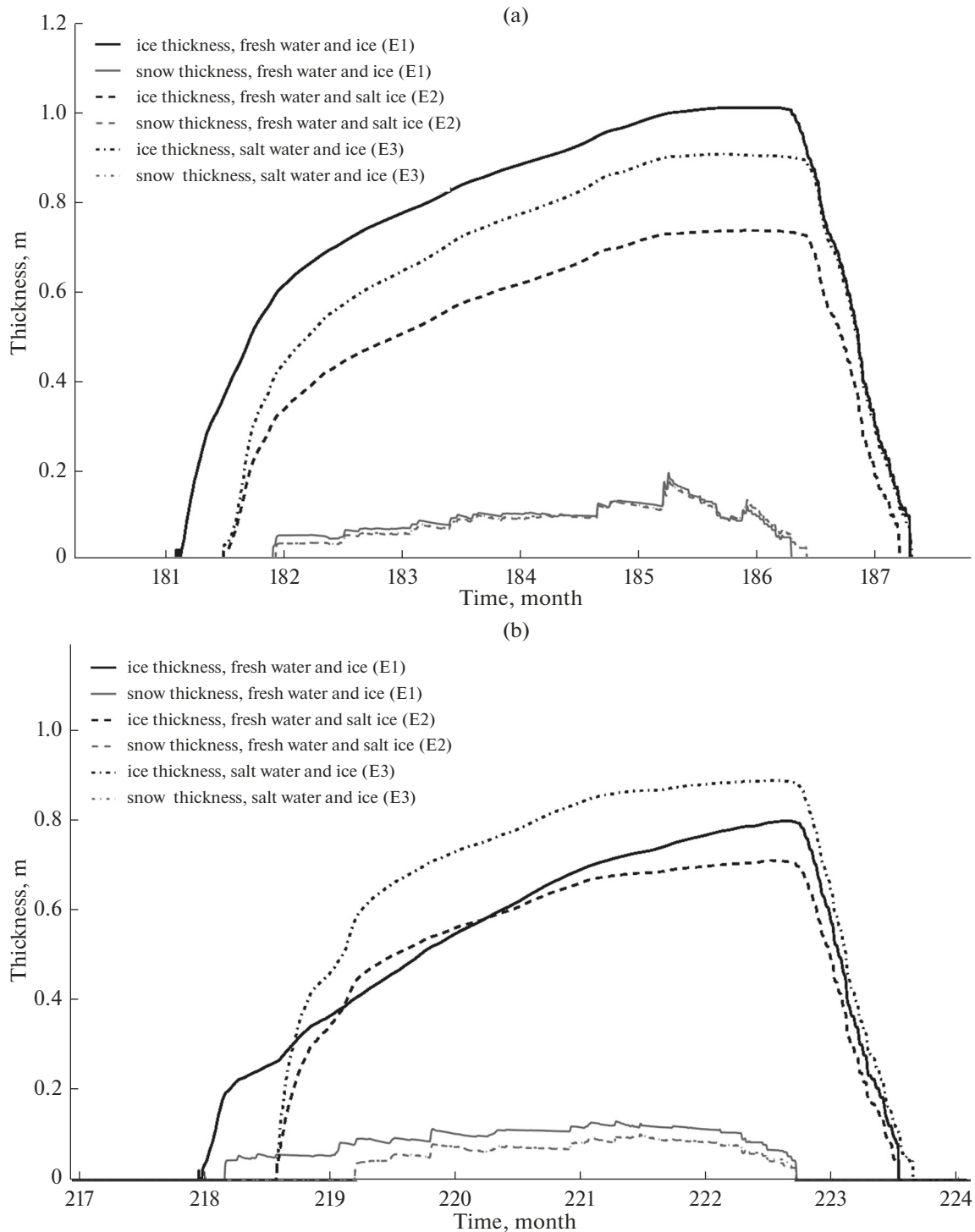
Fig. 2. Temporal evolution of the snow and ice thickness on Lake Uvs Nuur according to the new version of the LAKE model in three numerical experiments: E1, E2 and E3 (the setup of experiments is given in the main text). (a) Winter 1993–1994; (b) winter 1996–1997.

heat balance at the phase-transition boundary. That is, other factors being equal, the growth of salty ice is faster than freshwater ice, because water in this case does not freeze completely and is included in the volume of ice in the form of brine. Using parameters characteristic of the Uvs Nuur lake in formulas (8) it is easy to show that $p_0 \approx 0.27$ and $dh_{i1,\mathrm{E3}}/dh_{i1,\mathrm{E2}} \approx 1.37$. However, the ratio of ice thicknesses in these experiments is noticeably less than 1.37, since this effect is partially compensated by the fact that the thermal dif-

Table 2. Dates of ice-off and onset of ice cover at Lake Uvs Nuur according to satellite data (sat) (t1 is the beginning of ice thawing, t2 is complete ice-off, t3 is the beginning of ice cover formation, and t4 is full ice cover on the lake) and numerical experiments with the LAKE model (E1−E3) (t2 is the loss of the ice layer and t4 is the emergence of the ice layer). Errors of modeling of theice-on and ice-off dates: ME is the mean error and RMSE is the root-mean-square error. The comparison was carried out for the next dates: t2 (sat) and t2 (E1, E2, E3), t4 (sat) and t4 (E1, E2, E3)

Year	t1 (sat)	t2 (sat)	t2 (E1)	t2 (E2)	t2 (E3)	t3 (sat)	t4 (sat)	t4 (E1)	t4 (E2))	t4 (E3)
2000	1.05	12.05	15.05	8.05	12.05	19.11	25.11	16.11	6.1	4.12
2001	9.05	16.05	17.05	10.05	17.05	30.11	14.12	26.11	11.12	7.12
2002	11.05	19.05	25.05	17.05	24.05	28.11	11.12	3.12	20.12	5.12
2003	13.05	19.05	27.05	21.05	27.05			19.11	12.12	30.11
2004	11.05	10.05	20.05	13.05	20.05	24.11	8.12	21.11	12.12	13.12
2005	3.05	10.05	21.05	16.05	22.05	1.12	10.12	1.12	9.12	4.12
2006	15.05	24.05	21.05	20.05	21.05	4.12	15.12	26.11	15.12	24.12
2007	28.04	5.05	11.05	14.05	8.05	29.11	10.12	26.11	6.12	2.12
2008	11.05	19.05	22.05	18.05	21.05	3.12	15.12	1.12	13.12	15.12
2009	9.05	17.05	19.05	21.05	22.05	2.12	8.12	19.11	7.12	9.12
2010	12.05	21.05	31.05	30.05	1.06	8.12	15.12	4.12	12.12	9.12
2011	8.05	20.05	16.05	16.05	23.05	3.12	12.12	23.11	9.12	4.12
2012	8.05	22.05	15.05	16.05	16.05	28.11	9.12	27.11	5.12	5.12
2013	2.05	12.05	19.05	10.05	11.05	13.12	20.12	3.12	13.12	13.12
2014	6.05	18.05	22.05	15.05	18.05	30.11	13.12	29.11	12.12	7.12
2015	8.05	17.05	12.05	13.05	16.05	20.11	12.12	21.11	16.12	21.12
ME		0	3.3	−0.2	3.1		0	−16.7	−0.1	−1.7
MSE		0	6.1	4.9	5.9		0	18	4.8	6.6

fusivity for salt ice is less than for pure ice: using formulas (2)−(3), it can be shown that their ratio is 0.59−0.84 for ice porosity 0.1−0.3. Therefore, other factors being equal, the removal of heat upward from the phase transition boundary in the salty ice cover is slower. At the same time, the heat flux from the underlying water layers to the freezing front in experiments E2 and E3 differs slightly (8.4 and 9.3 W/m², respectively), which causes a small difference in the rate of ice growth.

The average winter maximum ice thickness for the period 1980−2015 in E3 experiment was 0.97 m (with standard deviation 0.16 m), which is in good agreement with the average value according to observations (0.98 m, [24]) while, without taking the salinity of ice into account (experiment E2), this value is significantly underestimated by the model (0.77 m). Note that, when using the constant ice salinity 4‰ in the model, the average maximum ice thickness was 0.80 m (with standard deviation 0.12 m), which is also noticeably less than in the more complete model and inthe measurement data.

The late date of ice−off in E3 is partly due to the early onset of ice (Table 2). The early onset of ice, in turn, is partially caused in the model by neglecting the destruction of thin ice cover forced by mesoscale atmospheric vortex over the lake. This vortex develops during cold air outbreaks from land on the relatively warm lake waters in the period preceding freezing. This effect is easily seen in satellite images. The model does not take into account also the fact that the ice begins to thaw in spring from the shores, where the depth of the lake is small and the heating by solar radiation is fast, and becomes covered with cracks over the entire area through which water can also rapidly heat up, accelerating the destruction of ice. The slow melting of ice in the model is also evidenced by the fact that, in the E3 calculation, the snow on the lake melts earlier than according to satellite observations by an average of 5−6 days (for the period of 2000−2017) and, thus, the ice-off after the disappearance of snow in the model is 9 days longer than in real conditions. In addition to the mentioned effect of partial destruction of ice, this may also be due to the inaccuracy of defining the radiation characteristics of ice (for example, the albedo, which varies from 0.2 to 0.9 for ice [8, 27, 33,], etc.)

It is curious to note that, in model experiments taking into account the salinity of water after the loss of snow cover and in the process of intensive thawing of ice, a desalinized zone and a very stable salinity stratification develops under the ice. At the same time, shortwave radiation penetrates through the ice cover and the maximum temperature is formed in the upper water layers—a phenomenon known for lakes in where the stratification is determined by salinity [40, 41].

CONCLUSIONS

A new version 2.1 of the one-dimensional LAKE model of thermo-hydrodynamics and biogeochemistry of the water reservoir is presented. The model is supplemented with a description of the dynamics and vertical distribution of salinity in the ice cover. The model is compared with the data of *in situ* and satellite measurements of temperature and ice cover on Uvs Nuur Lake (Mongolia) for 2000 to 2015.

It was shown that insufficient vertical mixing in the lake during the warm season in the model with the standard turbulent closure $k-\varepsilon$ leads to a significant shift in the ice-on dates. In this paper, this problem is solved by introducing an additional (background) coefficient of turbulent thermal conductance/diffusion into the models. It was also demonstrated that, if the salinity of the lake is neglected, the freeze-up according to the model starts $16-17$ days earlier than the actual dates. This error is removed if the model takes into account the influence of salinity of water on the density of water and the freezing point; however, at the same time, the model underestimates, on average, the maximum ice thickness during winter by ≈ 0.2 m. This error, in turn, is reduced by an order of magnitude if the model simulates the vertical distribution and the dynamics of salinity in ice. The traditional approach using a constant value of ice salinity does not provide such an effect. The remaining inaccuracies in simulating the ice cover can be attributed to the following effects not reflected in the model: the destruction of the thin ice cover in the autumn due to wind, accelerated heating of the reservoir in spring due to the presence of edges and cracks, and the temporal evolution of the radiation properties (primarily albedo) of snow and ice.

ACKNOWLEDGMENTS

REFERENCES

1. V. F. Brekhovskikh, *Hydrophysical Factors of the Formation of the Oxygen Regime in Water Bodies*, Ed. by V. K. Debol'skii and A. G. Kocharyan (Nauka, Moscow, 1988) [in Russian].

2. S. Greene, K. M. Walter Anthony, D. Archer, A. Sepulveda-Jauregui, and K. Martinez-Cruz, "Modeling the impediment of methane ebullition bubbles by seasonal lake ice," Biogeosciences **11** (23), 6791−6811 (2014).

3. G. A. Hodgkins, I. C. James Ii, and T. G. Huntington, "Historical changes in lake ice-out dates as indicators of climate change in New England, 1850−2000," Int. J. Climatol. **22**, 1819−1827 (2002).

4. R. Latifovic and D. Pouliot, "Analysis of climate change impacts on lake ice phenology in Canada using the historical satellite data record," Remote Sens. Environ. **106** (4), 492−507 (2007).

5. A. Oveisy and L. Boegman, "One-dimensional simulation of lake and ice dynamics during winter," J. Limnol. **73** (3) (2014). doi 10.4081/jlimnol.2014.903

6. D. V. Mironov, *Parameterization of Lakes in Numerical Weather Prediction. Part 1: Description of a Lake Model*, Tech. Rep. (Deutscher Wetterdienst, Offenbach, 2008).

7. X. Fang and H. G. Stefan, "Long-term lake water temperature and ice cover simulations/measurements," Cold Reg. Sci. Technol. **24** (3), 289−304 (1996).

8. M. Leppäranta, "Modelling the formation and decay of lake ice," in *The Impact of Climate Change on European Lakes* (Springer, Dordrecht, 2010), pp. 63−83.

9. L. C. Brown and C. R. Duguay, "Modelling lake ice phenology with an examination of satellite-detected subgrid cell variability," Adv. Meteorol. **2012**, 1−19 (2012).

10. A. F. Voevodin and T. B. Grankina, "Numerical simulation of the ice-cover growth dynamics in freshwater and brackish-water reservoirs," Mat. Zametki SVFU 147−158 (2012).

11. Yu. L. Nazintsev and V. V. Panov, *Phase Composition and Thermophysical Characteristics of Sea Ice* (Gidrometeoizdat, St. Petersburg, 2000) [in Russian].

12. N. G. Yakovlev, "Coupled model of ocean general circulation and sea ice evolution in the Arctic Ocean," Izv., Atmos. Ocean. Phys. **39** (3), 355−368 (2003).

13. P. J. Griewank and D. Notz, "A 1-D modelling study of Arctic sea-ice salinity," Cryosphere **9** (1), 305−329 (2015).

14. V. M. Stepanenko and V. N. Lykossov, "Numerical modeling of the heat and moisture transport in a lake−soil system," Russ. Meteorol. Hydrol. **30** (3), 69−77 (2005).

15. V. Stepanenko, I. Mammarella, A. Ojala, H. Miettinen, V. Lykosov, and T. Vesala, "LAKE 2.0: A model for temperature, methane, carbon dioxide and oxygen dynamics in lakes," Geosci. Model Dev. **9** (5), 1977−2006 (2016).

16. V. M. Stepanenko, E. E. Machul'skaya, M. V. Glagolev, and V. N. Lykossov, "Numerical modeling of methane emissions from lakes in the permafrost zone," Izv., Atmos. Ocean. Phys. **47** (2), 252−263 (2011).

17. V. M. Stepanenko, A. Martynov, S. Goyette, X. Fang, M. Perroud, and D. Mironov, "First steps of a lake model intercomparison project," Boreal Environ. Res. **15**, 191−202 (2010).

18. V. M. Stepanenko, A. Martynov, K. D. Jöhnk, Z. M. Subin, M. Perroud, X. Fang, F. Beyrich, D. Mironov, and S. Goyette, "A one-dimensional model intercomparison study of thermal regime of a shallow, turbid midlatitude lake," Geosci. Model Dev. **6** (4), 1337−1352 (2013).

19. V. Stepanenko, K. D. Jöhnk, E. Machulskaya, M. Perroud, Z. Subin, A. Nordbo, I. Mammarella, and D. Mironov, "Simulation of surface energy fluxes and stratification of a small boreal lake by a set of one-dimensional models," Tellus, Ser. A **66** (1), 21389 (2014).

20. W. Thiery, V. Stepanenko, X. Fang, K. Jöhnk, Z. Li, A. Martynov, M. Perroud, Z. Subin, F. Darchambeau, D. Mironov, and N. van Lipzig, "LakeMIP Kivu: Evaluating the representation of a large, deep tropical lake by a set of one-dimensional lake models," Tellus, Ser. A **66** (1), 21390 (2014).

21. P. V. Bogorodsky and A. V. Pnyushkov, "A simple model for seawater crystallization in the temperature spectrum," Oceanology (Engl. Transl.) **47** (4), 500−506 (2007).

22. O. M. Andreev and B. V. Ivanov, "Parametrization of the vertical distribution of first-year ice salinity for problems of thermodynamical modeling in the Arctic," Probl. Arkt. Antarkt. **75**, 99−105 (2007).

23. N. N. Zubov, *Arctic Ice* (Izd. Glavsevmorputi, Moscow, 1945) [in Russian].

24. M. Paul, PhD Thesis (Technische Universität, Dresden, 2012).

25. *The Recent Surface and Subsurface Waters in the Endorheic Uvs Nuur Basin (Northwest Mongolia)*, Ed. by W. Horn, M. Paul, D. Uhlmann, A. Dulmaa, G. Davaa, and N. Tseveendorj (S. Hirzel, Leipzig, 2016).

26. H. H. Poole and W. R. G. Atkins, "Photo-electric measurements of submarine illumination throughout the year," J. Mar. Biol. Assoc. U.K. **16** (1), 297−324 (1929).

27. D. K. Perovich, *The Optical Properties of Sea Ice*, Tech. Rep. (US Army Corps of Engineers, 1996).

28. P. Berrisford, D. P. Dee, P. Poli, R. Brugge, K. Fielding, M. Fuentes, P. W. Krallberg, S. Kobayashi, S. Uppala, and A. Simmons, *The ERA-Interim Archive version 2.0* (Shinfield Park, Reading, 2011).

29. S. N. MacCallum and C. J. Merchant, "Surface water temperature observations of large lakes by optimal estimation," Can. J. Remote Sens. **38** (1), 25−45 (2012).

30. K. Hosoda, H. Murakami, F. Sakaida, and H. Kawamura, "Algorithm and validation of sea surface temperature observation using MODIS sensors aboard terra and aqua in the western North Pacific," J. Oceanogr. **63** (2), 267−280 (2007).

31. S. Sharma, D. K. Gray, J. S. Read, C. M. O'Reilly, P. Schneider, A. Qudrat, C. Gries, S. Stefanoff, S. E. Hampton, S. Hook, J. D. Lenters, D. M. Livingstone, P. B. McIntyre, R. Adrian, M. G. Allan, O. Anneville, L. Arvola, J. Austin, J. Bailey, J. S. Baron, J. Brookes, Y. Chen, R. Daly, M. Dokulil, B. Dong, K. Ewing, E. de Eyto, D. Hamilton, K. Havens, S. Haydon, H. Hetzenauer, J. Heneberry, A. L. Hetherington, S. N. Higgins, E. Hixson, L. R. Izmest'eva, B. M. Jones, K. Kangur, P. Kasprzak, O. Koster, B. M. Kraemer, M. Kumagai, E. Kuusisto, G. Leshkevich, L. May, S. MacIntyre, D. Muller-Navarra, M. Naumenko, P. Noges, T. Noges, P. Niederhauser, R. P. North, A. M. Paterson, P.-D. Plisnier, A. Rigosi, A. Rimmer, M. Rogora, L. Rudstam, J. A. Rusak, N. Salmaso, N. R. Samal, D. E. Schindler, G. Schladow, S. R. Schmidt, T. Schultz, E. A. Silow, D. Straile, K. Teubner, P. Verburg, A. Voutilainen, A. Watkinson, G. A. Weyhenmeyer, C. E. Williamson, and K. H. Woo, "A global database of lake surface temperatures collected by *in situ* and satellite methods from 1985−2009," Sci. Data **2**, 150008 (2015).

32. I. V. Khvostov, A. N. Romanov, V. V. Tikhonov, and E. A. Sharkov, "Some features of microwave radiothermal radiation of freshwater reservoirs with ice cover," Sovrem. Probl. Distantsionnogo Zondirovaniya Zemli Kosmosa **14** (4), 149−154 (2017).

33. A. S. Gardner and M. J. Sharp, "A review of snow and ice albedo and the development of a new physically based broadband albedo parameterization," J. Geophys. Res. **115** (F1), F01009 (2010).

34. I. P. Chubarenko, *Horizontal Convection Above Underwater Slopes* (Terra-Baltika, Kaliningrad, 2010) [in Russian].

35. T. Arai, "Climatic and geomorphological influences on lake temperature," SIL Proc. **21** (1), 130−134 (1981).

36. K. Patalas, "Mid-summer mixing depths of lakes of different latitudes," SIL Proc. **22** (1), 97−102 (1922-2010).

37. A. Gaudard, R. Schwefel, L. R. Vinna, M. Schmid, A. Wuest, and D. Bouffard, "Optimizing the parameterization of deep mixing and internal seiches in one-dimensional hydrodynamic models: A case study with Simstrat v1.3," Geosci. Model Dev. **10** (9), 3411−3423 (2017).

38. H. Z. Baumert and H. Peters, "Turbulence closure: Turbulence, waves and the wave−turbulence transition − Part 1: Vanishing mean shear," Ocean Sci. **5** (1), 47−58 (2009).

39. M. Hondzo and H. G. Stefan, "Lake water temperature simulation model," J. Hydraul. Eng. **119** (11), 1251−1273 (1993).

40. G. Kirillin and A. Terzhevik, "Thermal instability in freshwater lakes under ice: Effect of salt gradients or solar radiation?," Cold Reg. Sci. Technol. **65** (2), 184−190 (2011).

41. V. Stepanenko, I. A. Repina, A. Artamonov, S. Gorin, V. N. Lykosov, and D. Kulyamin, "Mid-depth temperature maximum in an estuarine lake," Environ. Res. Lett. **13** (3), 035006 (2018).

Translated by M. Cherbunina